Macromolecular Research

Volume 16, Number 5 July 31, 2008

Feature Article

Application of Excited-State Intramolecular Proton Transfer (ESIPT) Principle to Functional Polymeric Materials

Sanghyuk Park, Sehoon Kim, Jangwon Seo, and Soo Young Park*

School of Materials Science and Engineering, Seoul National University, ENG 445, Seoul 151-744, Korea

Received May 7, 2008; Revised July 11, 2008; Accepted July 12, 2008

Abstract: Synthesis and properties of novel excited-state intramolecular proton transfer (ESIPT) materials, recently developed in our group, are described. Highly efficient ESIPT reaction, achieved in polyquinolines, polybenzoxazoles, and oxadiazole and imidazole derivatives possessing an intramolecular tautomerizable hydrogen bond, has been investigated theoretically and experimentally. It is demonstrated that unique properties arising from the ESIPT process (large Stokes' shift, no self-absorption, and easy population inversion, etc.) make it possible to produce advanced polymer devices for lasing, optical storage, and electroluminescence.

Keywords: fluorescence, excited-state intramolecular proton transfer, optical patterning, electroluminescence, amplified spontaneous emission.

Introduction

Excited-state intramolecular proton transfer (ESIPT) is a phototautomerization occurring in the excited states of the molecules possessing a cyclic intramolecular hydrogen bond.[1-5] It has been the research subject intensively studied in photochemistry and photophysics. As summarized in Scheme I, ESIPT-exhibiting molecules exist exclusively as an enol (E) form in the ground state, while upon photoexcitation, undergo tautomerization into a keto form (E*→K*) via an extremely fast and irreversible ESIPT process occurring in the sub-picosecond time regime. After the excited keto (K) form decays radiatively to the ground state keto (K) forms, the energy-wasting backward proton transfer occurs very readily restoring their initial enol forms, which is in general very efficient and thus has been applied to UV photostabilizers.[6] Moreover, different absorbing (E) and emitting (K*) species in the intrinsic four-level photocyclic scheme (E→E*→K*→K···) give rise to a large Stokes'-shifted fluorescence without self-reabsorption as well as an easy population inversion of the proton transferred keto form in the lowest excited state facilitating stimulated emission.[1-4] This peculiar characteristic has encouraged more novel applications including luminescent solar concentrators and proton transfer lasers.[5] Fluorescence probing is another promising application of ESIPT, due to its spectral sensitivity to environmental medium.[3,7,8,10]

In spite of these advantages, practical application of ESIPT has been limited by low emission efficiency and prominent concentration quenching of the keto emission. Accordingly, most of ESIPT phenomena have been investigated rather academically in dilute solution system, such as fluorescence

*Corresponding Authors. E-mail: parksy@snu.ac.kr

probe for molecular environment. Although several polymeric systems including simple blends or copolymers have been studied with an aim to realize solid lasers or electroluminescence, the tolerable contents of ESIPT-chromophore were far too low to achieve an aggregation-free and highly efficient solid-solution in polymeric matrix.[8,9] Recently, we have been successful in developing novel ESIPT molecules, polymers, and dendrimers with highly efficient fluorescence emission free from concentration quenching.[12-18] In this work, we provide a comprehensive summary of our recent achievements in the design and synthesis of novel ESIPT chromophores with specific focus on the amplified spontaneous emission, ESIPT photopatterning, and electroluminescence.

Theoretical Design of ESIPT Chromophore[7,11-12,22]

Structural prerequisite for ESIPT is an intramolecular hydrogen (H) bond that is built with acidic proton donor and basic proton acceptor (X–H···Y). In general, proton donor is hydroxyl group (X=O) and proton acceptor (Y) is basic nitrogen atom in heteroaromatic rings.[1-5] In this work, we selected quinoline, benzoxazole, and imidazole as a proton accepting heteroaromatic part. It is well known that those rings form acid-base complex and thus show processability in acidic solvents because nitrogen atom in these heteroaromatic rings is able to be protonated. This proton acceptability in turn, means that they can be employed for excited-state intramolecular proton transfer (ESIPT) when combined with intramolecular hydrogen (H) bond. On this basis, we designed a novel class of ESIPT chromophores (see Figure 1). Due to their six-membered intramolecular H-bonds, they are expected to have four-level photocyclic scheme driven by ESIPT, as shown in Scheme I.

We examined the feasibility of ESIPT in these chromophores with semiempirical molecular orbital calculation (PM3 parameter, MOPAC97).[11,22] In all the optimized geometries in four levels of ESIPT photocycle, each heterocyclic ring

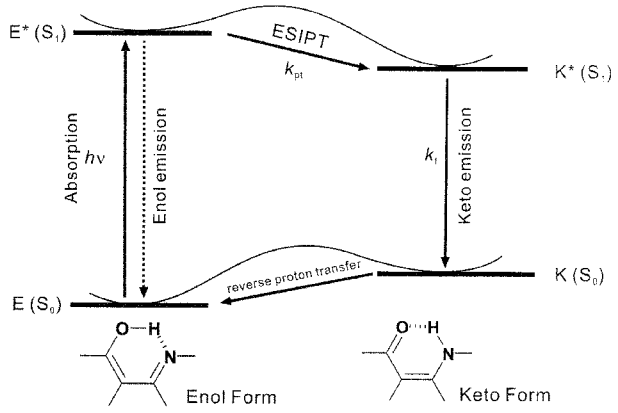

Scheme I. Schematic representation of ESIPT photocycle.

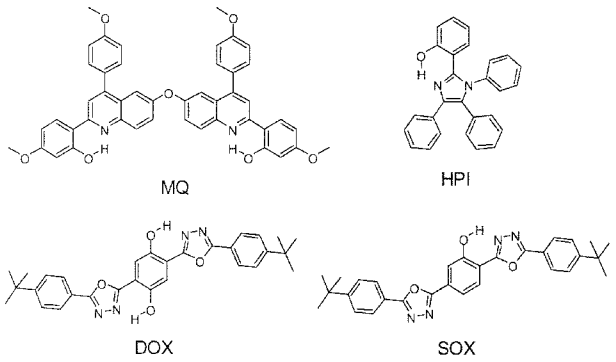

Figure 1. Molecular structures of novel ESIPT molecules.

and phenolic group, which form the cyclic intramolecular H bond, were found to be almost in-plane. Based on the reaction path obtained from calculated energies and bond lengths of normal enol form (N), tautomeric keto form (T), and transition state (TS) in the ground and the first excited singlet states, the occurrence of ESIPT was found to be energetically favorable. The enol form that is more stable than the keto form in the ground state becomes less stable in the excited state, bringing about a proton transfer to the excited keto form.

To realize compact and rugged devices with reliable performance, most of the ESIPT applications demand a highly dense solid-state system. However, as usual in common organic dyes, the intermolecular interaction between ESIPT molecules in the condensed phase is often associated with significant concentration quenching in the fluorescence intensity, which is a serious challenge to be addressed. Aiming at the high performance organic fluorescent materials in this work, we have introduced bulky side-groups into the molecules, i.e., twisted phenyl groups or dendritic structures (see Figures 1 and 4). It was initially considered that the bulky functional groups would favorably reduce the intermolecular vibronic interactions which would otherwise induce the non-radiative deactivation process.[16-18,22]

For practical applications of ESIPT fluorescence like in organic light emitting diodes (OLED), it is demanded that the emission color should be tuned over the whole range of visible light, from blue to red. In order to fulfill the requirement, we have designed and synthesized various kinds of heterocyclic compounds including imidazole,[22] oxadiazole,[29] and benzoxazole,[30] derivatives. By semiempirical molecular orbital (MO) calculations and subsequent organic syntheses, it was found that the emission colors show specific dependence on the nature of substituents. For example, the emission colors of HBO derivatives were shifted hypsochromically with electron donor and bathochromically with electron acceptor.[7] All together, novel ESIPT chromophores with intense fluorescence in solid state with tailored emission color could be obtained by proper design and synthesis

based on these theoretical considerations.[7,11-13,22]

ESIPT in Polymeric and Dendritic System[12,21,25-26,30]

The designed ESIPT chromophore MQ (see Figure 1) was incorporated into semi-rigid polyquinolines to investigate ESIPT in polymeric system (see Figure 2). PQH[12] and PQDH[23] retain the MQ structure in extremely high content, that is, in every second and every repeating unit of polymer backbone, respectively.[24] Polymerization was carried out by Friedländer reaction between bis(aminoketone) and OH-substituted bis(ketomethylene) monomers in the presence of P_2O_5 in m-cresol. PQH and PQDH showed excellent thermal stability with glass transition temperatures of 230 and 280 °C, respectively, and rather poor solubility in common organic solvents such as chloroform, tetrahydrofuran, dimethylformamide, and dimethylsulfoxide, etc. It is worth nothing that the reference polymer PQ is soluble in these organic solvents. The higher thermal stability and lower solubility of PQDH compared to PQH, are attributed to the increased rigidity and planarity of polymer backbone caused by the intramolecular hydrogen bonds in every repeating unit. However, both of these polymers showed good solubility in acidic solvents like formic acid, which is certainly assisted by acid-base complexation or protonation of quinoline moiety.

Figure 3(a) shows the static absorption and fluorescence spectra of PQ with alternating protic-aprotic units. Totally aprotic PQ (a H-bond free reference polymer) in tetrachloroethane (TCE) that are partially overlapping each other to show typical values of Stokes' shift. The absorption spectrum of PQH is structured similar to that of PQ and matches well with the calculated one. Except for the slight red shift of absorption edge, no remarkable difference was observed between the absorption spectra of PQH and PQ, implying that the electronic effect of OH-substitution is not significant in absorption. With respect to PL, however, the hydroxyl group exerts a noticeable influence, so that PQH solution shows an additional PL band besides the normal blue one (Figure 3(b)). This suggests an occurrence of ESIPT process in PQH. The blue band, when compared with the spectrum of aprotic PQ, may originate both from the aprotic unit and the E form of the protic unit. In the PQH film spin-coated from TCE solution as seen in Figure 3(c), the absorption

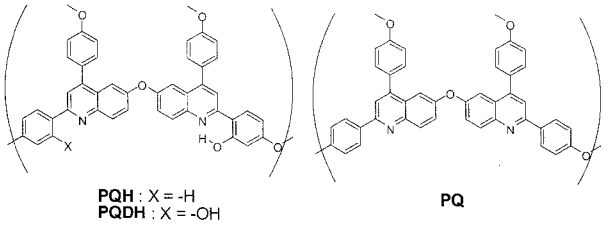

Figure 2. Structures of ESIPT-active polyquinolines (PQH and PQDH) and its reference polymer PQ.

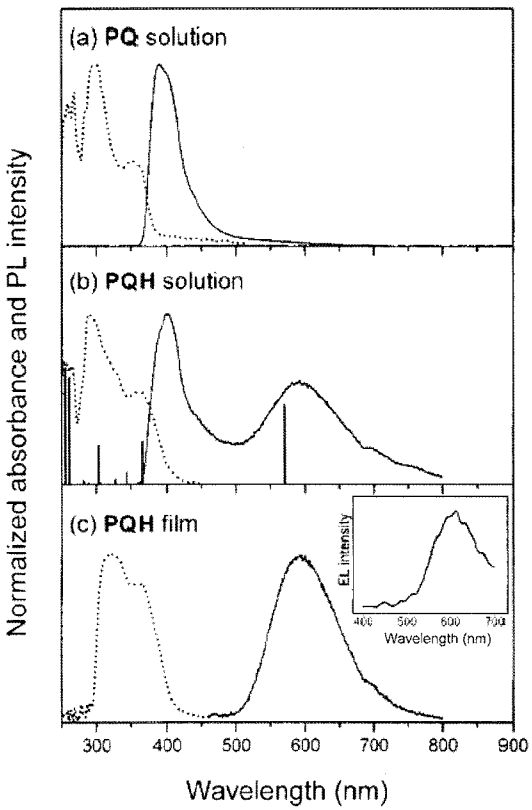

Figure 3. Absorption (dotted) and fluorescence (solid) spectra, excited at 310 nm, of PQ in TCE solution (a), PQH in TCE solution (b), and PQH film (c). Vertical lines in the absorption and the red fluorescence spectra of (b) indicate the corresponding calculated transition energies, respectively. The inset of (c) is the EL spectrum of a PQH single-layer device. Reproduced with permission from Ref. 12; Copyright 2000, American Chemical Society.

spectrum is the same as that of solution, while the blue PL band is totally quenched, giving only a strong red band. This suggests that ESIPT becomes much more efficient in film than in solution because the torsional motion is virtually frozen far below the glass transition temperature so that the H-bonded conformer is preferred energetically. Furthermore, no blue emission even from the aprotic unit indicates that the energy of the excited aprotic unit transfers completely to the protic unit of a lower energy followed by the occurrence of ESIPT. Electroluminescence (EL) spectrum from the device assembly of Al/PQH/ITO at 20 V also showed only the red band emission from K* (see the inset of Figure 3(c)): recombination of hole and electron generates N* exciton, which is subsequently transformed to K* via ESIPT process.

With an aim to obtain more effective solid medium with ESIPT fluorescence, dendritic structure was incorporated into the ESIPT system. Poly(aryl ether) dendrimers that are cored with phototautomerizable quinoline (QG*n*, *n*=1,2,3) were investigated since dendritic encapsulation strategy can

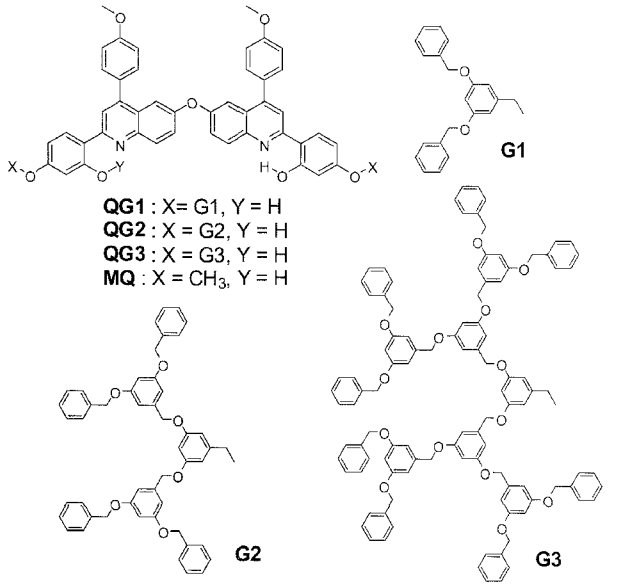

Figure 4. Low molecular mass (MQ) and dendritic molecules (QG*n*) based on phototautomerizable quinoline.

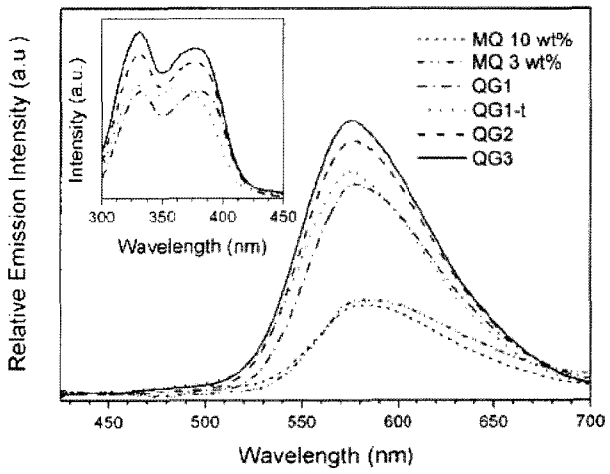

Figure 5. Relative emission intensities of QG*n* films and MQ-polystyrene blend films (3, 10 wt%), each spectrum obtained by excitation at 370 nm. The inset is the excitation spectra for the emission of QG*n* at 580 nm. Reproduced with permission from Ref. 26; Copyright 2002, American Chemical Society.

isolate fluorophores from each other to depress concentration quenching.[22,24] The photo-tautomerizable quinoline core was synthesized by Friedlander reaction between bis(aminoketone) monomer for PQDH and 2,2',4'-dihydroxyacetophenone, which was subsequently coupled with Frechet's archetypal poly(aryl ether) dendron to give QG*n*. All dendritic compounds QG*n* are glassy and formed scattering-free transparent film by spin-coating. The effect of dendrimer generation on the emission behavior was thoroughly studied for the film samples of QG*n*.[28,29]

All the QG*n* films emitted abnormally large Stokes shifted (~200 nm) orange fluorescence with no spectral overlap between absorption and emission, unambiguously arising from the fast and effective ESIPT in the film state. Certainly, this orange emission from QG*n* films is attributed to the characteristic fluorescence from the proton-transferred excited keto form (K*) of quinoline-based core. As mentioned above,[23] PQH solution gave dual emission from both enol and keto forms (ca. 400 and 590 nm, respectively) while the film gave only keto emission because the excited-state intramolecular proton transfer (ESIPT) in film was more effective than in solution most likely by the suppressed rotational motion in the solid film. Similar to PQH film, QG*n* films emitted no detectable fluorescence from the enol form in 360-500 nm, suggesting that the effective H-bond and the fast proton transfer are operating also in QG*n* films. Importantly, the relative emission intensity of QG*n* films, which was normalized by the absorbance at excitation wavelength of 370 nm, was increased with increasing number of phenyl rings in dendron shell, indicative of the improved efficiency of keto emission with increasing dendrimer generation. Moreover, all the dendritic compounds QG*n*, whose chromophore content in total weight is very high ranging from 18 wt% (QG3) to 54 wt% (QG1), showed much higher emission efficiency relative to that of non dendritic MQ in more dilute solid solution (3 and 10 wt% in polystyrene blend film) as shown in Figure 5. This is primarily due to the cooperative effect of dendritic shell that can actually separate the emitting core from each other to suppress the fluorescence quenching via molecular association. Therefore, it is proved that the ESIPT dendrimers are a new class of solid ESIPT medium with large content of active chromophores and efficient ESIPT emission.

Amplified Spontaneous Emission (ASE) from ESIPT Materials[16,22-25]

Due to the intrinsic four-level photocyclic process, stimulated emission (SE) assisted by population inversion could be readily observed from our ESIPT-active polymers, dendrimers, and single crystals when the pump energy exceeded certain threshold value.[19] Actual optical gain was observed in the transient photomodulation (PM) spectrum ($-\Delta T/T$) of PQDH film, obtained by pump-probe measurement using a femtosecond Ti:sappire laser system, where T is the probe transmission and ΔT is its transient modulation.[16,17,23] PM spectra of the PQDH film after various delay times comprised a negative band between 640 and 760 nm. This negative band can be assigned as "optical gain" by stimulated emission, where the delayed probe beam stimulates the emission from the proton transferred K* into K. The temporal profile of the optical gain at 660 nm showed exponential decay with rather fast time constant of below 20 ps. Com-

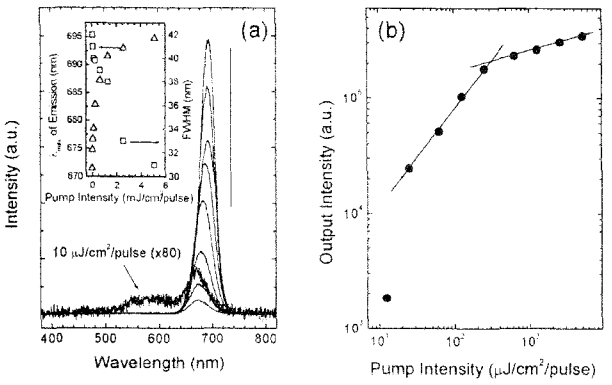

Figure 6. (a) Emission spectra of QG2 spun film (480 nm thick). The excitation intensity increases from 10 to 5,100 μJ/cm^2·pulse in the order indicated by the bold arrow. The inset shows the traces of λ_{max} and FWHM. (b) The dependence of the integrated emission intensity on the excitation intensity. Reproduced with permission from Ref. 27; Copyright 2002, American Chemical Society.

pared with the normal fluorescence lifetime of keto emission from PQH film (~300 ps), the faster decay of the optical gain indicates the rapid depletion of the excited-state population by stimulated emission. This finding clearly confirms that population inversion is easily achievable in the PQDH film due to the 4-level nature of ESIPT.

The emission amplification, particularly the amplified spontaneous emission (ASE) was readily observed in ESIPT dendrimer QG2(see Figure 6). When the QG2 film (480 nm thick) was excited by 355 nm picoseconds laser pulse with elliptical excitation area, the orange keto emission was guided and propagated along the longer axis of the excited region and amplified to generate the intense and narrow red ASE emission at 670~695 nm. In the high pumping region, the traces of the peak wavelength (λ_{max}) and the full width at half maximum (FWHM) have asymptotically approached to 695 and 31 nm, respectively. The threshold for amplification is lower than 20 μJ/cm^2/pulse, indicative of easy population inversion by intrinsic 4-level nature of ESIPT as well as the highly efficient dendritic effect for site-isolation.[22] The amplification in QG2 film is strongly influenced by waveguiding along and within the film plane, as shown by the emission anisotropy detected from the normal and edge sides of the film simultaneously. The gain amplification obtained only in the edge direction suggests that only the emission guided within the excited region of the film can be amplified by stimulated emission, which strongly supports ASE mechanism.

The ASE phenomenon was most effectively observed in a single crystal of ESIPT molecule, due to its well-ordered molecular structure and amplified optical gain as well as scattering-free propagation of stimulated emission along the surface of crystals.[20,22] Recently, we synthesized a novel class of imidazole-based ESIPT materials, i.e., hydroxy-substituted tetraphenyl imidazole (HPI) and its derivative HPI-Ac, which formed large single crystals exhibiting intense blue fluorescence and ASE. Transparent, clear, and well-defined fluorescent single crystals of HPI-Ac as large as 20 mm×25 mm×5 mm were easily grown from its dilute solution. From the X-ray crystallographic analysis and semi-empirical molecular orbital calculation, it was found that the four phenyl groups substituted in the imidazole ring of HPI and HPI-Ac allowed the crystals free from concentration quenching of fluorescence by limiting the excessive tight-stacking responsible for the intermolecular vibrational coupling and relevant non-radiative relaxation. Efficient ASE with spectral narrowing was observed in the HPI-Ac single crystal even at low excitation levels attributed to the intrinsic four-level ESIPT photocycle.[16,17,24] When the HPI-Ac single crystal sample was excited by a 355-nm picosecond pulse (~25 ps) with circular excitation area, the blue K* emission was amplified into the intense and narrow blue band. Figure 7(c) shows a spectral evolution as a function of the pump intensity, where the emission was collected from the edge of the crystal. The diameter of pump beam was 9 mm and the intensity was tuned from 0.11 to 3.5 mJ·cm^{-2} pulse^{-1} onto the sample without focusing. Even though the spectral narrowing was observed easily by the non-focused

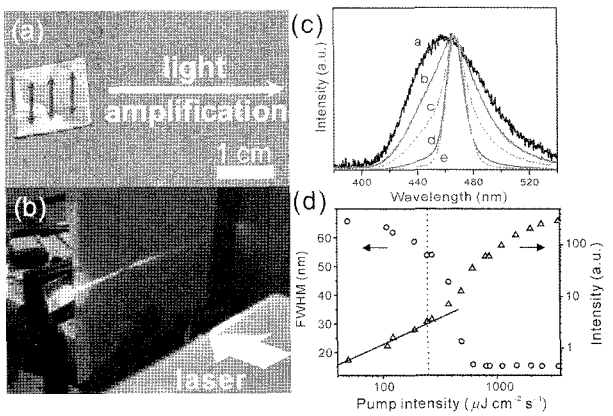

Figure 7. (a) Schematic representation of the optimal polarization direction in the HPI-Ac single crystal. (b) A photograph of a straight path, at the right angle to the photo-excitation, of blue ASE at the excitation fluence of 10 mJ·cm^{-2}pulse^{-1}. A cylindrical lens was used to shape the photo-excitation beam into a stripe with a width of approximately 500 μm and a length of 9 mm. (c) Peak-normalized emission spectra of a single crystal of HPI-Ac at various 355 nm pulse excitation energies of a) 0.11, b) 0.38, c) 0.49, d) 0.79, and e) 3.5 mJ·cm^{-2} pulse^{-1}. (d) The integrated emission intensity and FWHM of emission spectra, excited at 355 nm within circular area having diameter of 9 mm, of a single crystal of HPI-Ac as a function of pump energy. A solid line shows slope = 1. A dotted line shows the phenomenological threshold where ASE occurs. Reproduced with permission from Ref. 24; Copyright 2005, American Chemical Society.

beam, a loss of spectral narrowing was also monitored when the diameter of the pump beam was below a certain size, which is one of the characteristics associated with ASE.[28] The fluorescence emission and ASE of the sample shown in Figure 7 was collected in a direction perpendicular to the excitation beam under optimized geometry of polarization as shown in Figure 7(a). At a low pump fluence of 0.11 mJ cm^{-2} $pulse^{-1}$, the emission spectrum was initially very broad and the full width at half-maximum (FWHM) was approximately 67 nm. When the pump fluence was gradually increased, the FWHM decreased down to 13 nm in this system. In order to optimize the gain-narrowing condition, we used a cylindrical lens to form a line focus (500 μm × 9 mm, Figure 7(b)) on the front surface of the sample, and the polarization direction of the pump was varied with a half-wave plate. The gain-narrowing of HPI-Ac crystal was strongly dependent on the pump polarization, as expected. When the polarization was aligned parallel to the active chain orientation, the gain-narrowing was observed at lower pump fluence and FWHM was also decreased down to 9 nm. Figure 7(c) shows the evolution of the FWHM and the hyperlinear dependency of integrated emission for the HPI-Ac crystal as a function of pump intensity. It is noted that the emission intensity is approximately proportional to the pump fluence up to 250 μJ cm^{-2} $pulse^{-1}$, after which the characteristic hyperlinear dependence is clearly developed. The observation that the narrowing of line shape and hyperlinear dependence occur at the similar pump energy indicates that both effects are the results of light amplification at the wavelength where the single crystal has high gain. The onsets of significant spectral narrowing, which we will call the phenomenological threshold, were observed at around 200 μJ cm^{-2} $pulse^{-1}$ in non-focused state and at 6 μJ cm^{-2} $pulse^{-1}$ in the line-focused state, respectively. Above this "threshold", spontaneous emission from one emitter efficiently stimulates emission as it propagates along the excited region of the sample. Amplification occurs preferentially where the stimulated-emission cross-section is maximum, leading to gain narrowing.

Fluorescence Imaging by Photopatterning of ESIPT Materials[29,30]

Fluorescence imaging in polymer films is of growing interest owing to its potential application to optical recording.[29,30] To date, various organic fluorophores dispersed in or attached to polymer matrices have been used to achieve luminescence activation or deactivation by selective photochemical reaction. Most typical methodologies include photoacid-catalyzed chemical amplification and photoacid-induced protonation. Though a number of examples on photoacid-induced definition of fluorescent areas have been reported, the instability of the photopatterned image is one

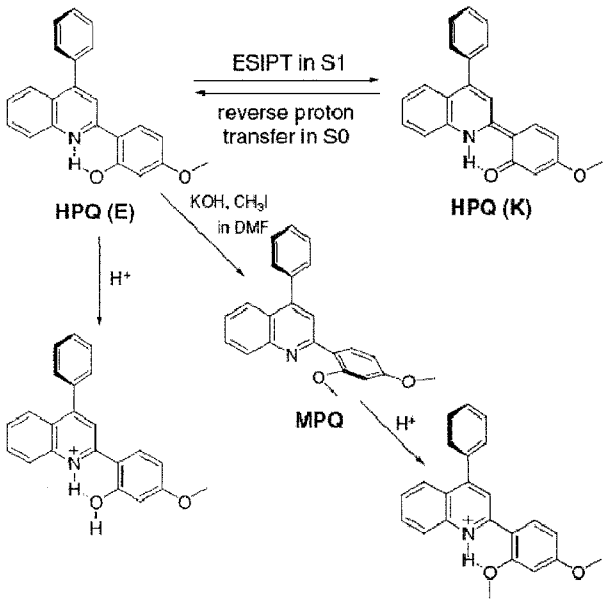

Scheme II. Structures of quinoline-based fluorophores related to methylation, protonation, and photochemical process. Dotted line in the molecular structure indicates H-bonds.

of the serious problems limiting their practical application. To solve this problem, we have designed a quinoline-based fluorophore (HPQ) with controlled basicity. The structure of HPQ is characterized by intramolecular hydrogen (H) bonding that is introduced to reduce basicity to extrinsic acid by intrinsic blocking of the acid-labile site, e.g., the nitrogen atom of quinoline. This is the key factor of stability enhancement of optically recorded images as a non H-bonding reference compound, MPQ was also synthesized as shown in Scheme II.

To investigate the readout stability, PMMA films of HPQ and MPQ with sufficient accessibility (PAG/fluorophore = 36 wt%/4 wt%) were irradiated at 349 nm (0.3 $mWcm^{-2}$) where both fluorophores held significance absorbance value while that of PAG was only marginal. In the case of H-bond-free MPQ, protonation progressed considerably even in less than 12 min, as is evident in the significant absorption change (see Figure 8(d)). In contrast, H-bonded HPQ almost retained its initial, unprotonated absorption, even after 120 min of irradiation, clearly demonstrating the fairly high readout stability of HPQ (see Figure 8(e)). The major reason for this stability is the difference of basicity between HPQ and MPQ. The other possible reason is excited-state inhibition of protonation by ESIPT (intramolecular acid-base reaction in the excited HPQ), or inhibition of photoacid generation by the excitation of HPQ, since the readout process involves the excitation of HPQ. The former can be excluded because protonation of HPQ did not occur even in the ground state in the post-exposure baking step with already-formed photoacid. Moreover, it was deduced that

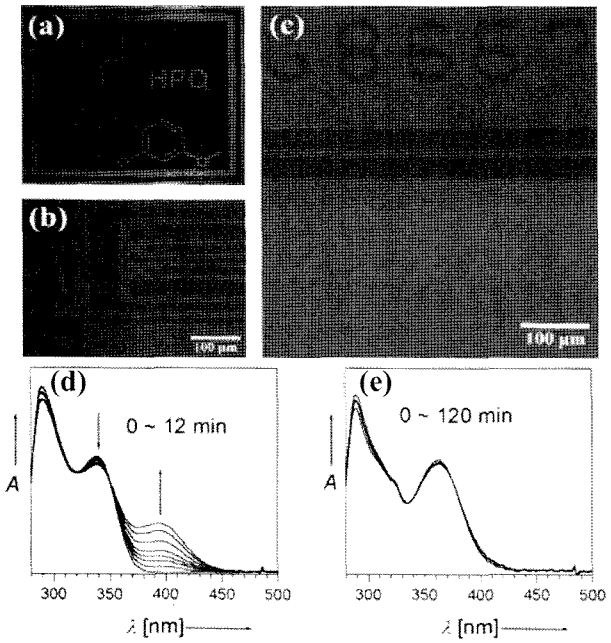

Figure 8. Fluorescence images of HPQ in PMMA films: (a) orange-green dual color image (2×2 cm) and (b) fluorescence micropattern. The greenish areas are irradiated parts at 254 nm through the photomask. (c) Comparison of the fluorescence images of HPQ (top) and MPQ (bottom) after 30 min of exposure to readout probe light (365 nm hand-held UV lamp, 1.2 mW·cm^{-2}). Photoacid-induced absorption changes of (d) MPQ and (e) HPQ in PMMA film (fluorophore: 4 wt%, PAG: 36 wt%) as a function of on irradiation time (349 nm, 0.3 mW·cm^{-2} probe light). Reproduced with permission from Ref. 29; Copyright 2003, Wiley-VCH Verlag GmbH & Co. KGaA.

HPQ has no inhibiting effect on photoacid generation by considering the photoacid-induced protonation of MPQ in the presence of HPQ in a PMMA film under the readout conditions. These considerations lead to the conclusion that the reduced basicity of HPQ resulting from intramolecular H-bonding kinetically limits the process of protonation in photoacid-deficient conditions and offers readout stability via photochemically gated protonation by the light which is selective for the recording (254 nm) and reading (>340 nm) processes.

In principle, all the comprise ESIPT molecules comprise proton donating part and accepting part that generate intramolecular H bond. We have been interested in the reversible blocking of the proton donating hydroxyl group, because it could alter the fluorescence emission due to the blocking of ESIPT process. Therefore, selective photochemical reaction of hydroxyl group in polymeric ESIPT system was supposed to show the fluorescence photopatterning. As for the polymer backbone, polybenzoxazoles (PBOs) are most interesting with their excellent mechanical, thermal, and various functional properties as well as good

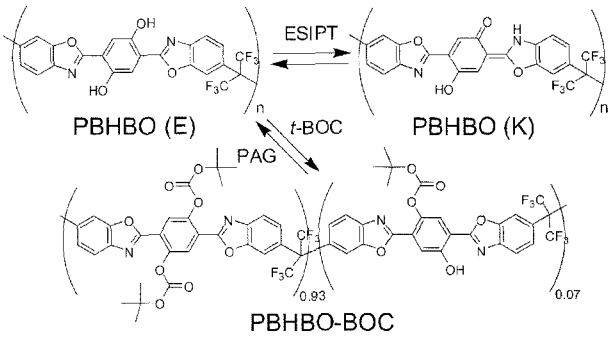

Scheme III. (a) Schematic diagram of the excited-state intramolecular proton transfer (ESIPT) in PBHBO and *t*-BOC blocking/deblocking conversions.

chemical resistance.[30] Due to the rigid molecular structure and consequent insolubility in organic solvents, however, fabrication and patterning of fine PBO films are seriously limited and remain as an important challenge. As shown in Scheme III, we have designed ESIPT-active PBO polymer (PBHBO), which comprises benzoxazole units and two aromatic hydroxyl groups virtually forming fused ring structures by cyclic intramolecular hydrogen (H) bonds, of which the hydroxyl groups are employed as the *t*-BOC attaching site.[39] It was expected that the *t*-BOC blocking of PBHBO would provide the polymer with both the enhanced solubility and fluorescence modulation.

As shown in Figure 9, PBHBO absorbs UV light ($\lambda_{max,abs}$ =364 nm) and emits dual fluorescence, composed of a weak E emission (E*→E; $\lambda_{max,em}$=470 nm) and a strong K emission (K*→K; $\lambda_{max,em}$=597 nm), exhibiting orange fluorescence overall. In contrast to the normal Stokes' shift (6195 cm^{-1}, 106 nm) of E emission, abnormally large Stokes' shift (10722 cm^{-1}, 233 nm) of K emission is certainly due to the ESIPT process leading to the generation of K* tautomer of PBHBO. On the other hand, *t*-BOC blocking of the ESIPT site in PBHBO must eliminate the K* generation and thus the normal blue fluorescence similar to E emission is expected to be left behind. Actually, PBHBO-BOC shows blue emission with slight green tail in diluted $CHCl_3$ solution (1×10^{-5} mol/L), while fabricated thin film shows dominant green emission ($\lambda_{max,em}$=524 nm, see the inset in Figure 9(a)) with trace of blue emission. Deblocking of *t*-BOC group from PBHBO-BOC and accompanied fluorescence modulation could be effected either by the acidic condition[32] or by the heat treatment.[33] First, the thermal cleavage of *t*-BOC group was optically monitored by the spectral changes of UV-visible absorbance as well as photoluminescence in PBHBO-BOC film, as shown in Figure 9(a). Upon annealing at 195 °C, the absorption band of PBHBO-BOC at 354 nm decreased and that of PBHBO at 400 nm increased gradually with two isosbestic points at 366 and 388 nm, supporting the idea of stepwise cleavage of the *t*-BOC group.

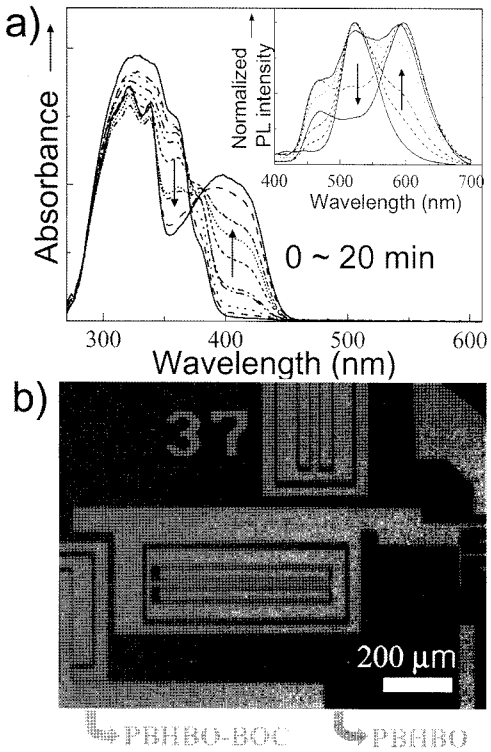

Figure 9. (a) Changes of UV-visible absorption spectra and emission spectra (inset) of PBHBO-BOC film depending on the annealing time at 195 °C. (b) Fluorescence micro-patterned image of PBHBO-BOC. The dark orange areas are the irradiated parts through the photomask. Reproduced with permission from Ref. 30; Copyright 2005, American Chemical Society.

For the fluorescence photopatterning of PBHBO-BOC film, chemical amplification resist method was employed for the *t*-BOC deblocking.[30] Polymeric thin film consisting of PBHBO-BOC and photo-acid generator (PAG, triphenylsulfonium trifluoromethanesulfonate, $\lambda_{max,abs}$=250 nm, PBHBO-BOC:PAG = 19:1 by weight), was spin-coated from chloroform solution. Upon irradiation with a hand-held UV lamp (1.2 mW cm^{-2}) through the photomask, the images were successfully transferred to the polymer film as the dual color fluorescence patterns as a result of the localized deblocking of *t*-BOC group (Figure 9(b)) in the irradiated parts. For the high contrast and fine resolution, post-exposure baking at 100 °C was carried out to ensure complete diffusion of generated photoacid.[29,30,34] It was also noted that the solubility difference between PBHBO and PBHBO-BOC was large enough to allow the fabrication of lithographic patterns.

Application of ESIPT Principles to the Efficient Blue and White Organic Light-emitting Diodes[21,35,36]

In order to achieve highly efficient organic light-emitting diodes (OLEDs) using luminescent molecules, synthesis of molecules with high luminescence quantum efficiency is essential.[37,38] Because of the ESIPT-active single molecules and polymers are basically fluorescent materials, they could be applied to OLED applications. Presently, efficient blue-emitting materials with excellent Commission Internationale de l'Eclairage (CIE) coordinates are still rare, and remain as an important challenge. Moreover, conventional luminescent organic molecules are limited by small Stokes' shift (normally less than 50 nm), giving rise to the self-absorption of their higher energy part emission spectrum, which not only reduces emission efficiency but also restricts lasing application seriously. Therefore, development of new blue emitting molecules with good color purity and high emission efficiencies as well as a large Stokes' shift is an important challenge. Fluorescent organic molecules exhibiting ESIPT process hold promising potentials in these respects.

Among our ESIPT molecules, hydroxyl-substituted tetraphenylimidazole (HPI) derivatives exhibiting intense blue fluorescence at 460 nm and low-threshold amplified spontaneous emission (ASE),[16-18,22] as discussed in Section IV, are considered to be promising as a blue emitter. However, practical fabrication of high efficiency OLEDs with them are seriously limited by the insufficient device stability related to the high degree of crystallinity of HPI molecules. Therefore, for the better OLED performance, proper structural modifications were strongly demanded to endow HPI with amorphous morphology and high glass transition temperature together with the improved charge carrier transport ability. Aiming at a highly efficient deep blue electroluminescence, we have designed and synthesized a novel class of HPI-based ESIPT materials covalently incorporating a structurally bulky and charge transporting functional groups (HPI-Cbz and HPI-Oxd, see Scheme IV), which, in fact, were found to be amorphous and highly fluorescent in the vacuum-deposited or spin coated thin film.[35]

HPI-Cbz and HPI-Oxd showed high T_g (~130 °C) and intense true blue emission (λ_{max}=462 and 468 nm, Φ_{PL}=0.44 and 0.38, respectively) with a large Stokes' shift (> 160 nm) and a narrow full width at half maximum (< 65 nm). Their

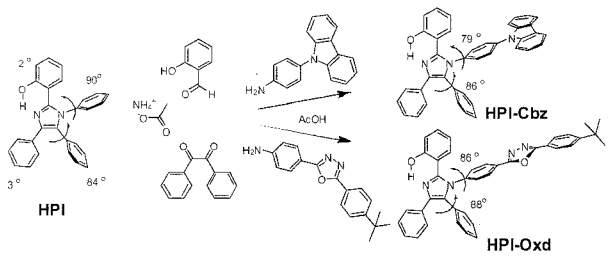

Scheme IV. Molecular structure of HPI and synthetic routes to the hydroxy-substituted tetraphenylimidazole derivatives, HPI-Cbz and HPI-Oxd.

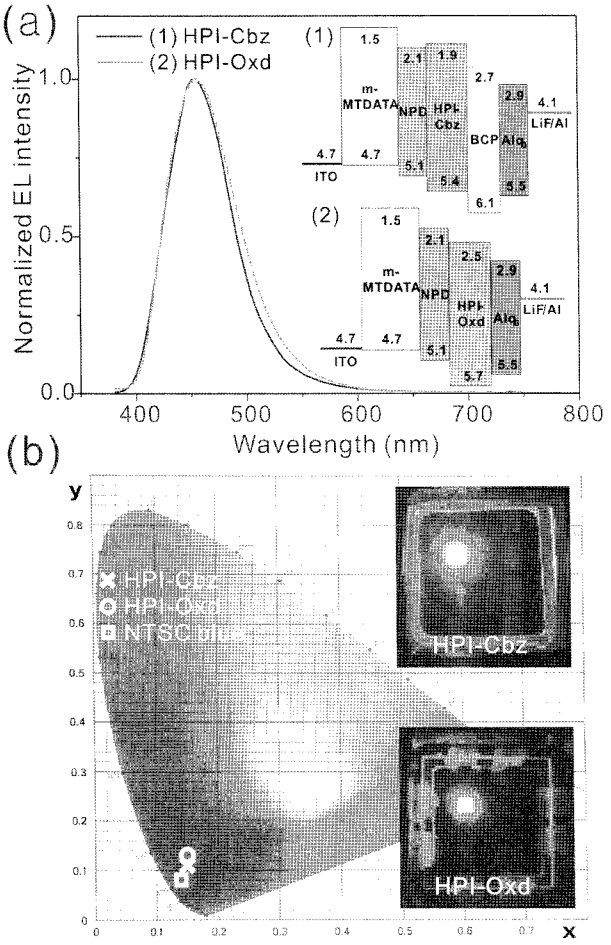

Figure 10. (a) Normalized electroluminescence spectra of (1) HPI-Cbz and (2) HPI-Oxd in different device structures at 10 mA/cm^2. Inset shows the device schematics of (1) ITO/*m*-MTDATA (50 nm)/NPD (20 nm)/HPI-Cbz (30 nm)/BCP (10 nm)/Alq_3 (20 nm)/LiF/Al (1/100 nm), (2) ITO/*m*-MTDATA (50 nm)/NPD (20 nm)/HPI-Oxd (30 nm)/Alq_3 (20 nm)/LiF/Al (1/100 nm). (b) Commission Internationale de l'Eclairage (CIE) coordinates and electroluminescence device operation photograph of HPI-Cbz and HPI-Oxd at 50 mA/cm^2. Reproduced with permission from Ref. 35; Copyright 2008, Wiley-VCH Verlag GmbH & Co. KGaA.

electroluminescent properties were investigated using a typical multi-layer device structure with hole-transporting layer (HTL) of *N,N'*-diphenyl-*N,N'*-bis(1-naphthalenyl)-(1,1'-biphenyl)-4,4'-diamine (NPD) and electron-transporting layer (ETL) of tris(8-hydroxyquinoline) aluminium (Alq_3). In the case of HPI-Cbz, the EL devices were fabricated with a configuration of ITO/*m*-MTDATA (50 nm)/NPD (20 nm)/HPI-Cbz (30 nm)/BCP (10 nm)/Alq_3 (20 nm)/LiF (1 nm)/Al (100 nm) (with *m*-MTDATA=4,4',4''-tris(3-methylphenylphenylamino) triphenylamine and BCP=2,9-dimethyl-4,7-diphenyl-[1,10]-phenanthroline), as depicted in Figure 10(a) (inset), together with their energy levels. The organic light-emitting devices using HPI-Cbz and HPI-Oxd as emitting layer generated an efficient blue electroluminescence (EL) emission peaking at around 460 nm with excellent CIE coordinates of (x, y)= (0.15, 0.11). A maximum external quantum efficiency of 2.94%, and a maximum brightness of 1,229 cd/m^2 at 100 mA/cm^2 as well as a low turn-on voltage of 4.8 V were achieved.

Another special application of ESIPT fluorescence is white luminescence generation from polymer films. White organic light-emitting diodes (WOLEDs) comprising organic and polymeric thin films are of growing interest in the lighting industry due to facile device fabrication and low power consumption. White luminescence, which covers the full spectral range of the visible region, is obtained by combining two or more fluorescence or phosphorescence colors from different emitting centers, because luminescence from a single organic compound is not broad enough. The simplest method is to use dye-dispersed polymer. However, the simple mixing of luminescent dopants in a polymer film can be a problematic as color balancing is difficult to control because of the undesirably dominant emission from the lower-bandgap dopants, even at very small amounts. This inherent problem arises from the inter-dopant Föster-type energy transfer between the higher bandgap donor and lower bandgap acceptor by means of spectral matching.

In spite of this difficulty, however, the energy-transfer problem was successfully solved by us by using the principle of ESIPT process. The most unique property of ESIPT system is a high energy UV absorption coupled with large Stokes' shifted visible emission resulting from fast ESIPT process (see Figure 11(a)). The lower-energy emitting tautomer (keto form) is efficiently generated upon the excitation of the higher-energy absorbing tautomer (enol form). In addition, by proper molecular design, ESIPT keto emission can be made more efficient and tuned over the whole range of the visible spectrum while keeping the absorption of their corresponding enol forms fixed in the UV region. Therefore, the homogeneous dispersion of two or more ESIPT dyes with different emission colors but in the same absorption spectra in a polymer matrix is expected to provide a simple fabrication method for a white-light emitting polymer film. This is attributed to the frustrated energy transfer caused by the unpopulated lower-energy emitter species as well as the spectral mismatch. Recently, we demonstrated the validity of this approach by mixing two different ESIPT dyes SOX and DOX with bluish-green (SOX) and orange (DOX) keto emissions in a polymer matrix (see Figure 1 for the chemical structure and Figure 11 for the spectra).[36]

As depicted in Figure 1, SOX and DOX have almost the same chemical structures, except for the number of hydroxyl groups, comprising a hydroxyl-substituted central phenyl unit and adjacent oxadiazole rings, which form cyclic intramolecular H bonds. Figure 11 shows the absorption and emission

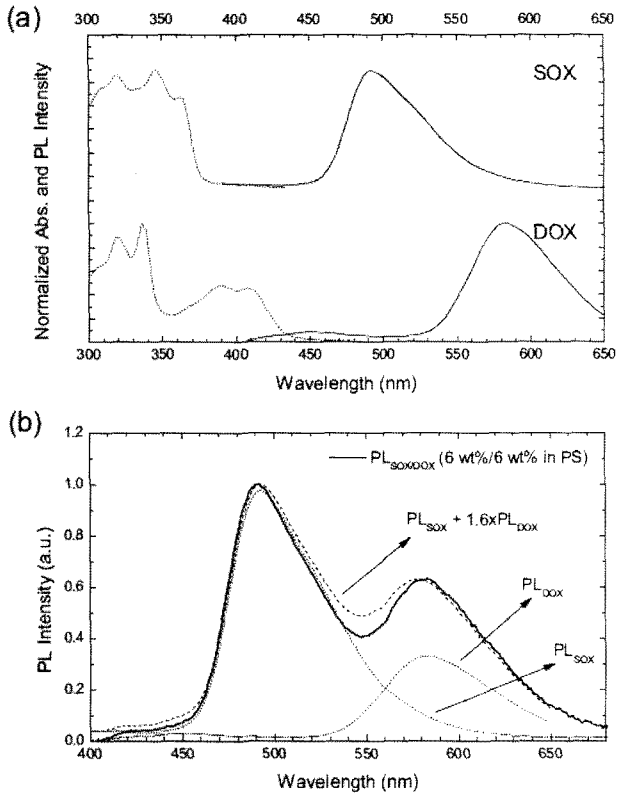

Figure 11. Absorption (dotted line) and photoluminescence spectra of SOX- and DOX-doped polystyrene films (6 wt% each). (b) Emission from SOX/DOX mixture (1:1 mixture) film excited at 365 nm. Dotted line indicate relative PL intensities of SOX and DOX films in Figure 11(a). Reproduced with permission from Ref. 36; Copyright 2005, Wiley-VCH Verlag GmbH & Co. KGaA.

spectra of SOX and DOX molecules, with characteristic large Stokes' shifts. The two molecules, dispersed in PS film, emitted a white light, implying that our strategy is working to make the system free from the energy transfer problem.

Efficient white-light emitting electroluminescence was achieved by using poly(*N*-vinylcarbazole) (PVK) as a blue-light-emitting and hole-transport polymer host. The structure of the studied EL device, fabricated by spin-casting, is ITO/poly(3,4-ethylenedioxythiophene):poly(styrene sulfonic acid) (PEDOT:PSS)/(ESIPT-dyes doped PVK)/Mg:Ag (9:1). This simple device showed bright white light emission with a maximum luminance of 1360 cdm^{-2} at 970 mA·cm^{-2} and a maximum external quantum efficiency of 0.06%. The CIE coordinates of the device were (x,y)=(0.29,0.31) and showed insignificant dependence of voltage between 8 and 13 V (Figure 12). By optimization of EL device structure with different SOX:DOX ratio and addition of BCP layer, the device IV (SOX:DOX ratio=9:1) showed a maximum luminance of 3,100 cdm^{-2} at 660 mA·cm^{-2}, with a maximum quantum efficiency of 0.26% and emission efficiency of 1.3 cdA^{-1}.

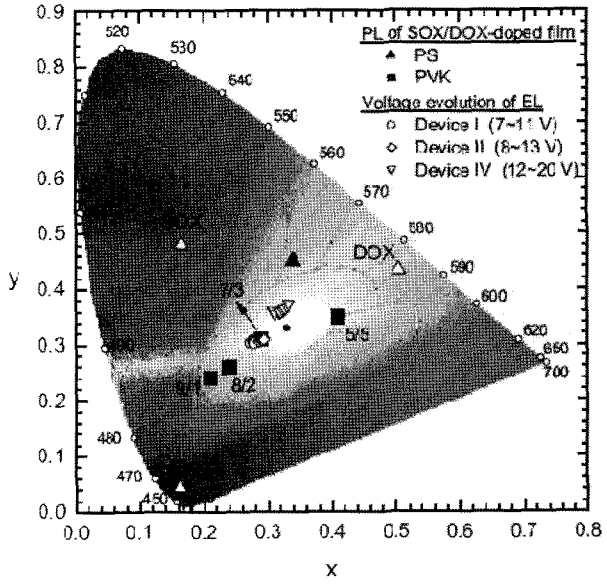

Figure 12. Emission colors in the CIE chromaticity diagram. The inner oval and the filled circle (0.33, 0.33) indicate the whitish region and the ideal white color, respectively. SOX:DOX ratio in device I and II is 7:3 and in device IV is 9:1 by weight, respectively. Reproduced with permission from Ref. 36; Copyright 2005, Wiley-VCH Verlag GmbH & Co. KGaA.

Summary

Novel class of ESIPT molecules based on heteroaromatic ring systems have been theoretically designed and synthesized. By proper molecular design, intense fluorescence emission in solid state were achieved, with the emission color tuned over the extended range of visible light. Attributed to the intrinsic 4-level nature of ESIPT photophysical process, stimulated emission and amplified spontaneous emission (ASE) were efficiently demonstrated from ESIPT materials including polymers, dendrimers, and single crystals. Using the protonation/deprotonation strategy and photochemical reaction of functional hydroxyl group in ESIPT fluorophore, the fluorescence photopatterning for optical memory were demonstrated in polymer films. Furthermore, efficient blue and white organic light-emitting diodes were successfully fabricated, taking advantage of the characteristic large Stokes' shift of ESIPT fluorescent materials.

Acknowledgment. This review article is based on several years of research on synthesis and application of excited-state intramolecular proton transfer (ESIPT) materials performed at Molecular Photonics Laboratory, Seoul National University. This work was supported by the Korea Science and Engineering Foundation (KOSEF) through the National Research Lab. Program funded by the Ministry of Science and Technology (No.2006-03246).

References

(1) J. Goodman and L. E. Brus, *J. Am. Chem. Soc.*, **100**, 7472 (1978).
(2) M. Kasha, *Journal of the Chemical Society-Faraday Transactions Ii*, **82**, 2379 (1986).
(3) A. S. Klymchenko and A. P. Demchenko, *J. Am. Chem. Soc.*, **124**, 12372 (2002).
(4) K. Sakai, M. Ichikawa, and Y. Taniguchi, *Chem. Phys. Lett.*, **420**, 405 (2006).
(5) R. M. Tarkka, X. J. Zhang, and S. A. Jenekhe, *J. Am. Chem. Soc.*, **118**, 9438 (1996).
(6) M. Luiz, A. Biasutti, A. T. Soltermann, and N. A. Garcia, *Polym. Degrad. Stab.*, **63**, 447 (1999).
(7) J. Seo, S. Kim, S. Park, and S. Y. Park, *Bull. Korean Chem. Soc.*, **26**, 1706 (2005).
(8) R. Traiphol and 1N. Charoenthai, *Macromol. Res.*, **16**, 224 (2008).
(9) Y. H. Kim, H. O. Lee, and K.S. Lee, *Macromol. Res.*, **11**, 471 (2003).
(10) M. Fischer and P. Wan, *J. Am. Chem. Soc.*, **121**, 4555 (1999).
(11) J. Seo, S. Kim, and S. Y. Park, *J. Am. Chem. Soc.*, **126**, 11154 (2004).
(12) D. W. Chang, S. Kim, S. Y. Park, H. Yu, and D.-J. Jang, *Macromolecules*, **33**, 7223 (2000).
(13) C. H. Kim, D. W. Chang, S. Kim, S. Y. Park, and T. Joo, *Chem. Phys. Lett.*, **450**, 302 (2008).
(14) J. Seo, S. Kim, S. H. Gihm, C. R. Park, and S. Y. Park, *J. Mater. Chem.*, **17**, 5052 (2007).
(15) S. Park, O.-H. Kwon, Y.-S. Lee, D.-J. Jang, and S. Y. Park, *J. Phys. Chem.*, **111**, 9649 (2007).
(16) M. K. Nayak, J. Seo, S. Park, and S. Y. Park, *J. Photochem. Photobiol. A: Chem.*, **191**, 228 (2007).
(17) J. Seo, S. Kim, Y.-S. Lee, O.-H. Kwon, K. H. Park, S. Y. Choi, D.-J. Jang, and S. Y. Park, *J. Photochem. Photobiol. A: Chem.*, **191**, 51 (2007).
(18) H. H. Lim, S. Boomadevi, O.-Y. Jeon, K. Kyhm, M. Cha, S. Park, and S. Y. Park, *J. Kor. Phys. Soc.*, **50**, 484 (2007).
(19) H. H. Lim, S. Boomadevi, O.-Y. Jeon, K. Kyhm, M. Cha, S. Park, and S. Y. Park, *Mater. Lett.*, **61**, 4213 (2007).
(20) J. H. Park, O.-Y. Jeon, H. H. Lim, M. Cha, S. Park, and S. Y. Park, *J. Kor. Phys. Soc.*, **49**, S592 (2006).
(21) S. Kim, D. W. Chang, S. Y. Park, K. Kim, and J.-I. Jin, *Bull. Kor. Chem. Soc.*, **22**, 1407 (2001).
(22) C. Park, M. Rhue, and M. Im, *Macromol. Res.*, **15**, 688 (2007).
(23) S. J. Min, B. J. Park, and J. M. Kim. *Macromol. Res.*, **12**, 615 (2004).
(24) S. Park, O.-H. Kwon, S. Kim, S. Park, M.-G. Choi, M.-Cha, D.-J. Jang, and S. Y. Park, *J. Am. Chem. Soc.*, **127**, 10070 (2005).
(25) S. Kim, D. W. Chang, S. Y. Park, S. C. Jeoung, and D. Kim, *Macromolecules*, **15**, 6064 (2002).
(26) S. Kim, D. W. Chang, S. Y. Park, H. Kawai, and T. Nagamura, *Macromolecules*, **35**, 2748 (2002).
(27) S. Kim, S. Y. Park, I. Yoshida, H. Kawai, and T. Nagamura, *J. Phys. Chem. B.*, **106**, 9291 (2002).
(28) P.-T.Chou, Y.-C. Chen, W.-S. Yu, Y.-H. Chou, C.-Y. Wei, and Y.-M. Cheng, *J. Phys. Chem. A*, **105**, 1731 (2001).
(29) S. Kim and S. Y. Park, *Adv. Mater.*, **15**, 1341 (2003).
(30) S. Park, S. Kim, J. Seo, and S. Y. Park, *Macromolecules*, **38**, 4557 (2005).
(31) G. W. Kim, W. G. Jun, S. K. Lee, M. J. Cho, J. I. Jin, and D. H. Choi, *Macromol. Res.*, **13**, 477 (2005).
(32) C. S. Hong, M. Jikei, R. Kikuchi, and M. Kakimoto, *Macromolecules*, **36**, 3174 (2003).
(33) C.-W. Lee, Y-.H. Seo, and S.-H. Lee, *Macromolecules*, **37**, 4070 (2004).
(34) J, M. Klopp, D. Pasini, J. D. Byers, C. G..Willson, and J. M. Fréchet, *Chem. Mater.*, **13**, 4147 (2001).
(35) S. Park, J. Seo, S. H. Kim, and S. Y. Park, *Adv. Funct. Mater.*, **18**, 726 (2008).
(36) S. Kim, J. Seo, H. K. Jung, J.-J. Kim, and S. Y. Park, *Adv. Mater.*, **17**, 2077 (2005).
(37) I. B. Berlman, *Handbook of Fluorescence Spectra of Aromatic Molecules*, Academic Press, New York, 1971.
(38) J. C. deMello, H. F Wittmann, and R. H. Friend, *Adv. Mater.*, **9**, 230 (1997).
(39) J. Yoo, J. H. Lee, I. Cho, K. D. Ahn, and J. M. Kim, *Macromol. Res.*, **11**, 69 (2003).